UNIVERSITY AT STONY BROOK

CEAS Technical Report 696

THREE-DIMENSIONAL CORNER SINGULARITIES IN VLSI CAPACITANCE ESTIMATION

Yimin Zhang and A. H. Zemanian

This work was supported by the National Science Foundation under Grants MIP-9200748 and DMS-9200738.

July 22, 1994

Three-Dimensional Corner Singularities In VLSI Capacitance Estimation [1]

YIMIN ZHANG and A. H. ZEMANIAN

Department of Electrical Engineering

State University of New York at Stony Brook

Stony Brook, N. Y. 11794-2350

Abstract

A significant problem in the computation of capacitances coefficients for VLSI interconnection and other electromagnetic transmission systems is caused by the singularities in the electric field at the corners and edges of conductors. For two-dimensional models, a solution is given by the so called "Duncan Correction", which is based on a polar expansion of the field. No such exact expansion exists in the three-dimensional case. Recent research has led to some appropriate asymptotic expressions for those singularities, and these are used to derive algorithms for correcting conventional capacitance computation. This correcting factor accounts for the singularities at the corners of the conductors. Finally we present a few examples to illustrate the three-dimensional capacitance correction procedure and computational accuracy.

[1]This research was support by the National Science Foundation under Grants MIP-9200748 and DMS-9200738

I Introduction

This paper concerns the "interconnection lines of interconnection network". One common category of such networks consists of the interconnection circuits on a VLSI chip; other such systems are power transmission networks and microwave striplines.

Much work has been done in the computation of capacitance coefficients for two-dimensional models of interconnection lines and other conducting bodies, but much less has been accomplished for three-dimensional models. See [5], [6], [8], [9], [15], [17], [20]-[25], [27]-[30], [32],[34]. A major difficulty in the computation of capacitance coefficients arises from singularities in the electrical field at the three-dimensional corners of a conductor. There are also field singularities along the edges of conductors, but their contributions to capacitance coefficients are readily determined by Duncan's correction [7], [32], which is based upon an exact polar expansion of the field. Since no such exact expansion exists in spherical coordinates, there is no exact three-dimensional analog of the Duncan Correction. Instead, we have sought an approximating asymptotic expression for the electrical field near a three-dimensional reentrant corner. There is a literature on this subject, see [2]-[4], [11]-[13], [16], [18], [19]. Much of this work is of a very general nature dealing with a variety of differential equations and a variety of geometries. The paper of Beagle and Whiteman [3] appears to be the most pertinent one for our purposes. By using the results of that work, we construct a correction factor for capacitance of three-dimensional conductors. The factor accounts for the singularities at the corners of the conductors.

II Two-dimensional Capacitance Corrections

In order to calculate capacitance we first solved the Laplace equation using a finite-difference method. However, this method is less accurate in the vicinity of a conductor's reentrant corner because of a singularity in the electric field at the corner. Duncan [7] corrects much of the resulting error for a two-dimensional corner by using a series approximation for the electrical potential in that vicinity. As is illustrated in Figure 1. He chooses a polar coordinate system with the origin at the center. In our examples. $\theta_0 = 3\pi/2$. Moreover, we shall choose the nodal array such that a node exists at the corner and the array's axes are parallel to the conductor's surface.

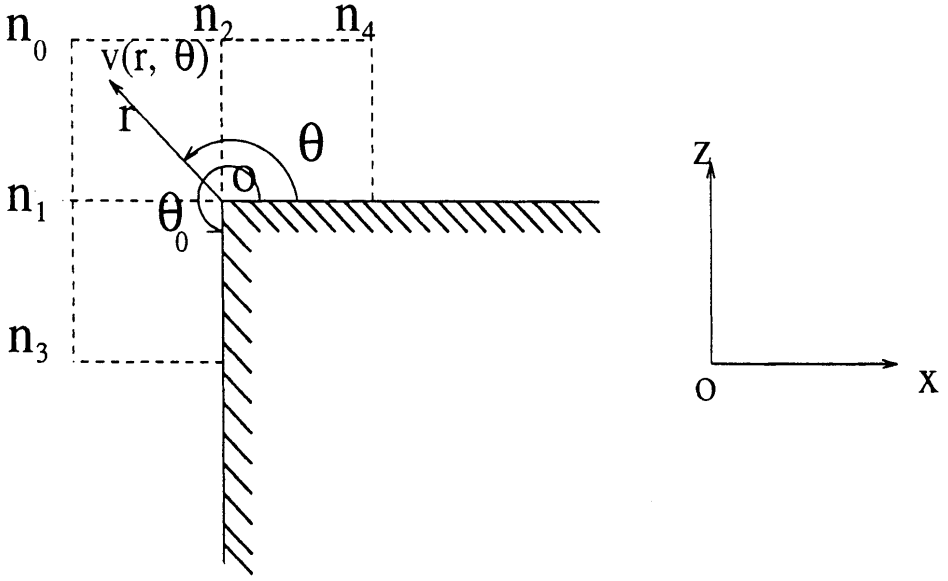

Figure 1: A two-dimensional corner.

According to the Duncan correction, we have

$$V(r,\theta) = V_0 + \sum_{m=1}^{\infty} a_m r^{m\pi/\theta_0} \sin(m\pi\theta/\theta_0) \tag{1}$$

If we sample (1) at M points in the vicinity of the corner node, we can determine the coefficients a_m for the truncated series expansion for the electrical potential:

$$V(r,\theta) = V_0 + \sum_{m=1}^{M} a_m r^{m\pi/\theta_0} \sin(m\pi\theta/\theta_0) \tag{2}$$

In particular, since we have computed $V(r,\theta)$ at several nodes in the vicinity of the corner through our finite-difference analysis, we can substitute M of those values into (2) to determine approximately $a_1,\ldots,a_M$. Next, the normal component of ∇V along the conductor's surface can be determined by differentiating (2), which in turn determines the normal component of the electric flux density along the surface. By integrating the latter quantity along the surface from $-\Delta z/2$ to the origin and then to $\Delta x/2$ (see Figure 1), we finally obtain the charge at that part of the corner.

Now let's get the corrected charge for the two-dimensional corner. In Figure 1, along the surface at $\theta = 0$ and for $r = \sqrt{x^2+z^2}, z = r\sin\theta$, we have

$$\begin{cases} \frac{\partial r}{\partial z} = \frac{z}{\sqrt{x^2+z^2}} = \sin\theta \\ \partial z = \partial r \sin\theta + r\cos\theta\partial\theta \\ 1 = \frac{\partial r}{\partial z}\sin\theta + r\cos\theta\frac{\partial\theta}{\partial z} \\ \frac{\partial\theta}{\partial z} = \frac{\cos\theta}{r} \end{cases} \tag{3}$$

Therefore,

$$\begin{aligned} \frac{\partial V}{\partial n} &= \frac{\partial V}{\partial z} = \frac{\partial V}{\partial r}\frac{\partial r}{\partial z} + \frac{\partial V}{\partial\theta}\frac{\partial\theta}{\partial z} \\ &= \frac{\partial V}{\partial r}\sin\theta + \frac{\partial V}{\partial\theta}\frac{\cos\theta}{r} \\ &= \sum_{m=1}^{M} a_m \frac{m\pi}{\theta_0} r^{\frac{m\pi}{\theta_0}-1}\cos\left[\theta(1-\frac{m\pi}{\theta_0})\right] \end{aligned} \tag{4}$$

Hence,

$$\frac{\partial V}{\partial n}|_{\theta=0} = \sum_{m=1}^{M} a_m \frac{m\pi}{\theta_0} r^{\frac{m\pi}{\theta_0}-1} \tag{5}$$

Note that $r = x$; so, the charge Q_{top} on the top surface between 0 and $\frac{\Delta x}{2}$ is

$$\begin{aligned} Q_{top} &= -\epsilon\int_0^{\frac{\Delta x}{2}} \frac{\partial V}{\partial n}|_{\theta=0} dx \\ &= -\epsilon\sum_{m=1}^{M} a_m \left(\frac{\Delta x}{2}\right)^{\frac{2m}{3}} \end{aligned} \tag{6}$$

where ϵ is dielectric constant, and $\epsilon = 8.85 * 10^{12}$ farad/m in a vacuum. Also for the side

surface at $\theta = \frac{3\pi}{2}$ and noting that $r = \sqrt{x^2 + z^2}$, $x = r\cos\theta$, we have

$$\begin{cases} \frac{\partial r}{\partial x} = \frac{x}{\sqrt{x^2+z^2}} = \cos\theta \\ \partial x = \partial r \cos\theta - r\sin\theta\partial\theta \\ 1 = \frac{\partial r}{\partial x}\cos\theta - r\sin\theta\frac{\partial\theta}{\partial x} \\ \frac{\partial\theta}{\partial x} = -\frac{\sin\theta}{r} \end{cases} \tag{7}$$

Therefore,

$$\begin{aligned} \frac{\partial V}{\partial n} &= -\frac{\partial V}{\partial x} = -\left(\frac{\partial V}{\partial r}\frac{\partial r}{\partial x} + \frac{\partial V}{\partial\theta}\frac{\partial\theta}{\partial x}\right) \\ &= -\frac{\partial V}{\partial r}\cos\theta + \frac{\partial V}{\partial\theta}\frac{\sin\theta}{r} \end{aligned} \tag{8}$$

At $\theta = \frac{3\pi}{2}$, $\cos\theta = 0$, $\sin\theta = -1$; therefore

$$\begin{aligned} \frac{\partial V}{\partial n}|_{\theta=\frac{3\pi}{2}} &= -\frac{\partial V}{\partial\theta}\frac{1}{r} \\ &= -\sum_{m=1}^{M} a_m r^{\frac{m\pi}{\theta_0}-1}\cos\left(\frac{m\pi\theta_0}{\theta_0}\right)\frac{m\pi}{\theta_0} \\ &= -\sum_{m=1}^{M} a_m r^{\frac{m\pi}{\theta_0}-1}(-1)^m\frac{2}{3}m \end{aligned} \tag{9}$$

Note that r=z; so, the charge Q_{side} on the side surface between 0 and $-\frac{\Delta z}{2}$ is

$$\begin{aligned} Q_{side} &= -\epsilon\int_0^{\frac{-\Delta z}{2}} \frac{\partial V}{\partial n}|_{\theta=\frac{3\pi}{2}} dz \\ &= \epsilon\sum_{m=1}^{M} a_m(-1)^m\left(\frac{-\Delta z}{2}\right)^{\frac{2m}{3}} \end{aligned} \tag{10}$$

Thus the total corrected charge Q_{total} at the two-dimensional corner node is

$$\begin{aligned} Q_{total} &= Q_{top} + Q_{side} \\ &= \epsilon\sum_{m=1}^{M} a_m\left[-(\frac{\Delta x}{2})^{\frac{2m}{3}} + (-1)^m(\frac{-\Delta z}{2})^{\frac{2m}{3}}\right] \end{aligned} \tag{11}$$

We shall refer to this as the M-point Duncan correction since we have matched (2) at M points to obtain the first M coefficients a_m.

How does the Duncan correction affect our computed capacitance coefficients? By choosing each corner as a node in our nodel array and using symmetric differences to compute the

incremental capacitors of the grid, we in fact overestimated a conductor's edges because the incremental capacitors at each corner node extend beyond the conductor's corner. Hence we have assigned too much charge to the conductor. One possible correction is to reduce those corner incremental capacitors so that they do not extend beyond the edges, but this underestimates the total capacitance because the finite-difference method doesn't adequately account for the singularity in the electric field. The Duncan correction yields a capacitance value in between these two estimates.

III Three-dimensional Capacitance Corrections

We have conducted investigations into computationally efficient means of determining capacitance coefficients for three-dimensional models of interconnection lines and other conducting bodies.

A major difficulty in the computation of capacitance coefficients arises from singularities in the electrical field at the three-dimensional corners of a conductor. Since there is no exact three-dimensional expansion for the electric field, there is no exact three-dimensional analog of the Duncan correction. Instead, we have sought an approximating asymptotic expression for the electrical field near a three-dimensional reentrant corner. By following some ideas in [2], we construct a correction procedure for the field singularities at the corners of three-dimensional conductors as follows.

The coordinate system: We wish to compute the surface charge density in the vicinity of a three-dimensional rectangular corner of a conductor. For our asymptotic analysis, we can assume that the corner configuration extends to infinite. We also assume that the conductor is held at 1V and that the electric field decays to 0 as infinite is approached outside the conductor. We choose spherical coordinates (r, θ, ϕ) with the principle axis passing through the vertex of the corner and remaining equidistant from the three edges of the corner. This is illustrated in Figure 2. A unit sphere centered at the origin will intersect the three plane surfaces of the corner along a curve Γ. We choose our coordinate system such that ϕ equals

0°. 120°, and 240° at the three points where the edges of the corner meet the unit sphere. On Γ, the minimum value of θ is 125.26° and occurs at those three edge points. Also, on Γ, the maximum value of θ is 144.74° and occurs where ϕ equals 60°, 180° and 300°.

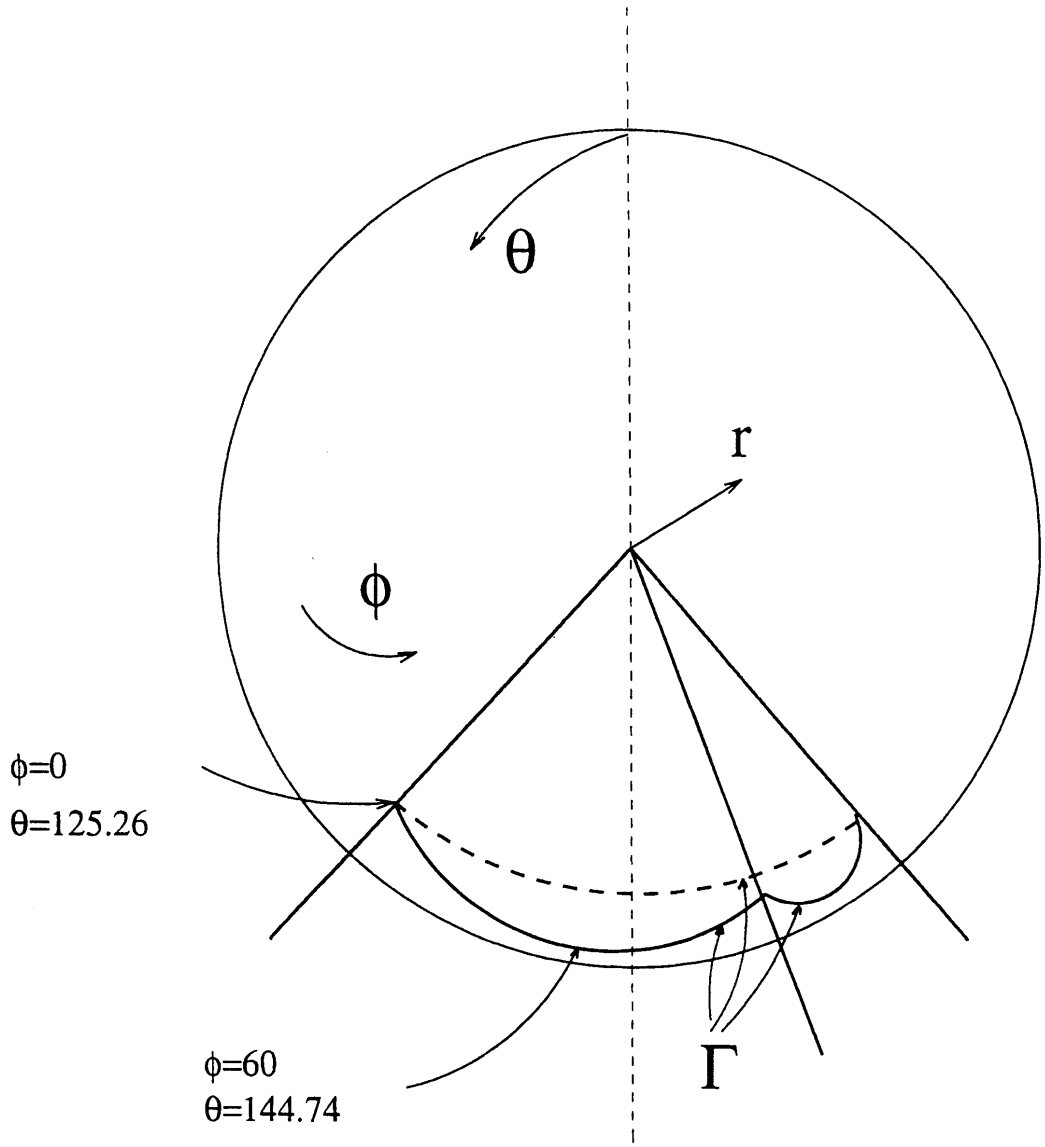

Figure 2: Intersection between a three-dimensional rectangular corner and the unit sphere.

Surface charge density: According to [3], an approximate asymptotic expression for the

potential in the vicinity of the corner is

$$V(r,\theta,\phi) = 1 + r^{\alpha} \sum_{n=0}^{N-1} a_n \cos 3no P_{\alpha}^{-3n}(\cos\theta) \tag{12}$$

It is shown in Appendix A that (12) satisfies the Laplace equation. Moreover we note that the range of α is in [0, 1]. Indeed, for $\alpha < 0$, the potential $V(r,\theta,\phi) \to \infty$ as $r \to 0$, which contradicts our boundary condition at $r = 0$. Also, for $\alpha > 1$, the electrical field $\to 0$ as $r \to 0$; this does not account for the field singularity in the vicinity of the corner.

In (12), $P_{\alpha}^{-3n}(\cos\theta)$ is the associated Legendre function of the first kind of degree α and order $-3n$. An appropriate value for α depends on the chosen value of N; it is estimated at α=.461 for N=2. as will be described later. $\vec{a} = [a_0, a_1, ..., a_{N-1}]^T$ is the eigenvector of B^{α} corresponding to the zero eigenvalue, where B^{α} is a certain singular N × N matrix which is chosen as indicated below.

For N=2, we have

$$V(r,\theta,\phi) \approx 1 + r^{.461}[a_0 P_{.461}^{0}(\cos\theta) + a_1 \cos 3\phi P_{.461}^{-3}(\cos\theta)] \tag{13}$$

Therefore, the surface charge density will be

$$\sigma = \varepsilon E_n = -\varepsilon \frac{\partial V}{\partial n} \tag{14}$$

where in the MKS units we have $\varepsilon = 8.85 \times 10^{-12}$ farad/m for a vacuum and

$$\frac{\partial V}{\partial n} = \frac{\partial V}{\partial r}\cos\gamma_{nr} + \frac{\partial V}{r\partial\theta}\cos\gamma_{n\theta} + \frac{\partial V}{r\sin\theta\partial\phi}\cos\gamma_{n\phi} \tag{15}$$

From Figure 3, we have

$$\begin{cases} \gamma_{nr} = 90° \\ \gamma_{n\theta} = -180° \\ \gamma_{n\phi} = 90° \end{cases} \tag{16}$$

where the γ's are the angles between the outward normal unit vector 1_n and the three coordinate unit vectors. Substituting (16) into (15), we get

$$\frac{\partial V}{\partial n} = -\frac{\partial V}{r\partial\theta} \tag{17}$$

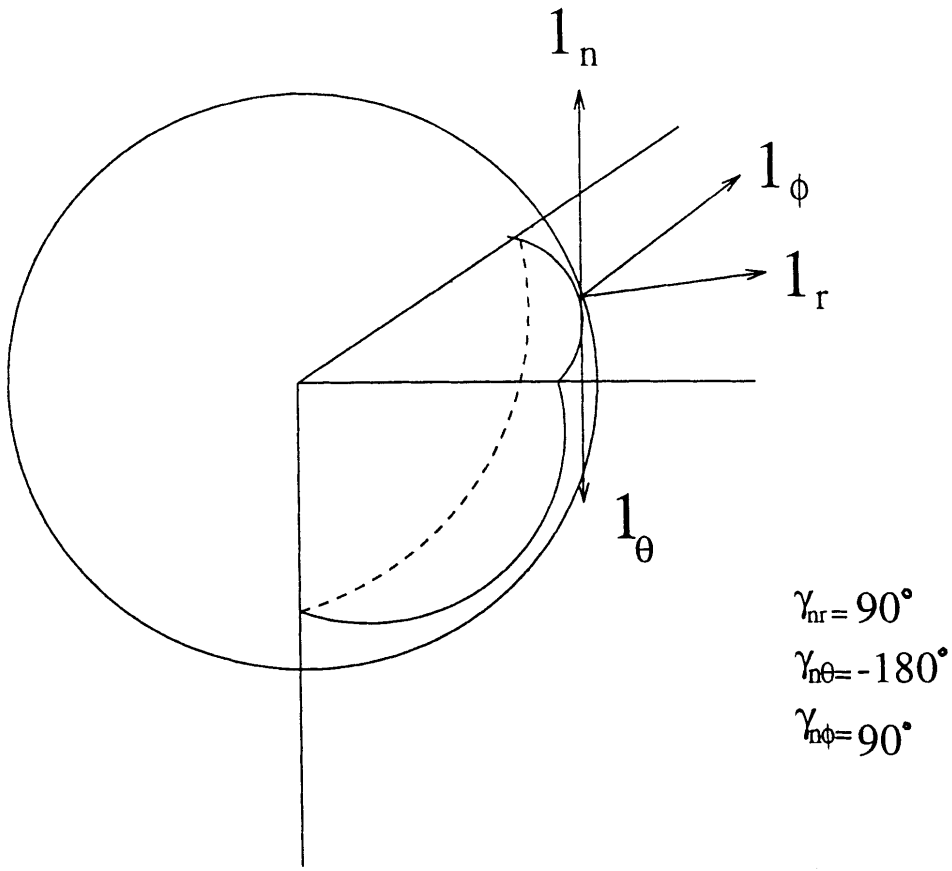

Figure 3: Angles between unit vectors.

From (13), (14) and (17), we have

$$\sigma = \varepsilon r^{-.539}[a_0 \frac{\partial P^0_{.461}(\cos\theta)}{\partial\theta} + a_1 \cos 3\phi \frac{\partial P^{-3}_{.461}(\cos\theta)}{\partial\theta}] \tag{18}$$

Let $\cos\theta = x$ and $dx = -\sin\theta d\theta$

$$\sigma = -\varepsilon r^{-.539} \sin\theta [a_0 \frac{\partial P^0_{.461}(x)}{\partial x} + a_1 \cos 3\phi \frac{\partial P^{-3}_{.461}(x)}{\partial x}] \tag{19}$$

From [10, page 161] for $-1 < x < 1$, we have

$$\frac{dP^\mu_\nu(x)}{dx} = \frac{1}{(1-x^2)}[(\nu+1)xP^\mu_\nu(x) - (\nu-\mu+1)P^\mu_{\nu+1}(x)] \tag{20}$$

According to (20), the surface charge density (19) becomes

$$\sigma = -\frac{\varepsilon r^{-.539}}{\sin\theta}\{1.461 a_0[\cos\theta P^0_{.461}(\cos\theta) - P^0_{1.461}(\cos\theta)] + a_1 \cos 3\phi[1.461\cos\theta P^{-3}_{.461}(\cos\theta) - 4.461 P^{-3}_{1.461}(\cos\theta)]\} \tag{21}$$

Determination of the eigenvector $\vec{\mathbf{a}}$ *with N=2:* Noting that the conductor is at 1 volt, we see that the summation in (12) should be zero, i.e.,

$$r^{\alpha} \sum_{n=0}^{N-1} a_n \cos 3n\phi P_{\alpha}^{-3n}(\cos\theta) \approx 0 \tag{22}$$

For each point on curve Γ in Figure 2, ϕ and θ are determined and this yields a linear equation in the a_n obtained by equating that summation to zero. Upon choosing N different points on the curve Γ between the points where $\phi = 0°$ and $\phi = 60°$, we obtain N simultaneous equations. With r=1, they may be written in matrix form as

$$B^{\alpha}\vec{\mathbf{a}} = 0 \tag{23}$$

where $\vec{\mathbf{a}}$ is the vector of coefficients $[a_0, a_1, \ldots, a_{N-1}]^T$ and B^{α} is an $N \times N$ matrix obtained by collocating N points along curve Γ in such a fashion that B^{α} is singular. This yields a nontrivial solution for $\vec{\mathbf{a}}$, namely, the eigenvector for the zero eigenvalue. As mentioned above, at the present time we have chosen N=2 and set $\alpha = 0.461$. To find values for a_i and α, we collocate at two points $\psi_0(\theta_0, \phi_0)$, $\psi_1(\theta_1, \phi_1)$ on curve Γ. Pairs(θ, ϕ) for points on the curve Γ can be given parametrically in terms of a variable ψ in the interval $[0, \pi/4]$ as follows.

$$\begin{cases} \cos\theta = -\sqrt{2/3}\sin(\psi + \pi/4) \\ \cos\phi = \frac{\sqrt{3}\cos\psi + \cos\theta}{\sqrt{2}\sin\theta} \qquad\qquad \psi \in [0, \pi/4] \end{cases} \tag{24}$$

See an Appendix B for the derivation of (24). From (22) we have

$$\begin{cases} a_0 P_{\alpha}^{0}(\cos\theta_0) + a_1 \cos 3\phi_0 P_{\alpha}^{-3}(\cos\theta_0) = 0 \\ a_0 P_{\alpha}^{1}(\cos\theta_1) + a_1 \cos 3\phi_1 P_{\alpha}^{-3}(\cos\theta_1) = 0 \end{cases} \tag{25}$$

We express (25) in matrix form

$$\begin{bmatrix} P_{\alpha}^{0}(\cos\theta_0) & \cos 3\phi_0 P_{\alpha}^{-3}(\cos\theta_0) \\ P_{\alpha}^{0}(\cos\theta_1) & \cos 3\phi_1 P_{\alpha}^{-3}(\cos\theta_1) \end{bmatrix} \begin{bmatrix} a_0 \\ a_1 \end{bmatrix} = 0 \tag{26}$$

Therefore

$$B^{\alpha} = \begin{bmatrix} B_{00}^{\alpha} & B_{01}^{\alpha} \\ B_{10}^{\alpha} & B_{11}^{\alpha} \end{bmatrix} = \begin{bmatrix} P_{\alpha}^{0}(\cos\theta_0) & \cos 3\phi_0 P_{\alpha}^{-3}(\cos\theta_0) \\ P_{\alpha}^{1}(\cos\theta_1) & \cos 3\phi_1 P_{\alpha}^{-3}(\cos\theta_1) \end{bmatrix} \tag{27}$$

Assuming that det $B^\alpha = 0$, we get $B^\alpha_{00}B^\alpha_{11} = B^\alpha_{10}B^\alpha_{01}$. From (25), the expression for the eigenvector is

$$\vec{a} = \begin{bmatrix} a_0 \\ a_1 \end{bmatrix} = a_0 \begin{bmatrix} 1 \\ -\frac{B^\alpha_{00}}{B^\alpha_{01}} \end{bmatrix} = a_0 \begin{bmatrix} 1 \\ -\frac{B^\alpha_{10}}{B^\alpha_{11}} \end{bmatrix} \tag{28}$$

For (25) to have a non-trivial solution we require that the determinant det B^α for $N = 2$ remains as close to 0 as possible as (θ, ϕ) range over Γ between the points $(\theta, \phi) = (0°, 125.26°)$ and $(\theta, \phi) = (60°, 144.74°)$. To this end, we choose α in the interval $0 \leq \alpha \leq 1$ to minimize the maximum value of det B^α over the said range for (θ, ϕ). This was done numerically. We took increments of .001 for α and computed max { det B^α:$(\theta, \phi) \in \Gamma$ }. The smallest of those maxima occured when $\alpha = .461$. See Figure 4.

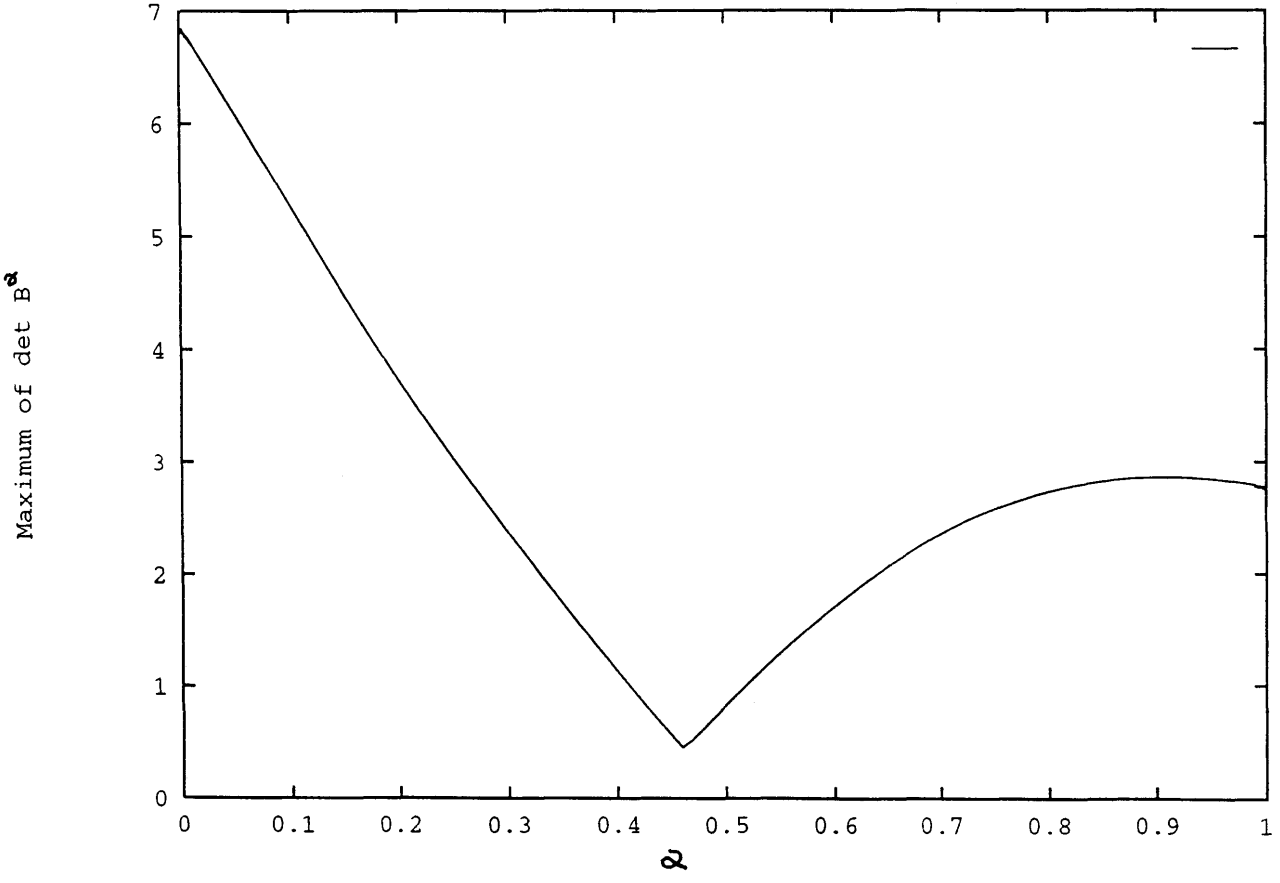

Figure 4: Maximum value of detB^α on curve Γ for various value of α.

Having determined α in this way, we now wish to determine the eigenvector $\vec{\mathbf{a}} = (a_0, a_1)$ for the eigenvalue 0 to within an arbitary constant. That is , we now want $(1, a_1/a_0)$ as the solution of $B^\alpha \vec{\mathbf{a}} = 0$, using a_0 as the arbitary constant. (a_0 in turn will be determined by matching the potential value at a point off the conductor but near the apex of the corner.) To pick up the best value of a_1/a_0 we consider the function

$$F(a_1/a_0, \psi) = P^0_{.461}(\cos\theta) + \frac{a_1}{a_0}\cos 3\phi P^{-3}_{.461}(\cos\theta)$$

we calculate its L_1, L_2 and L_∞ norm respectively, for various value of a_1/a_0. We found the smallest value of these norms occurred at the same value $a_1/a_0 = -0.05$. See Figures 5, 6, and 7.

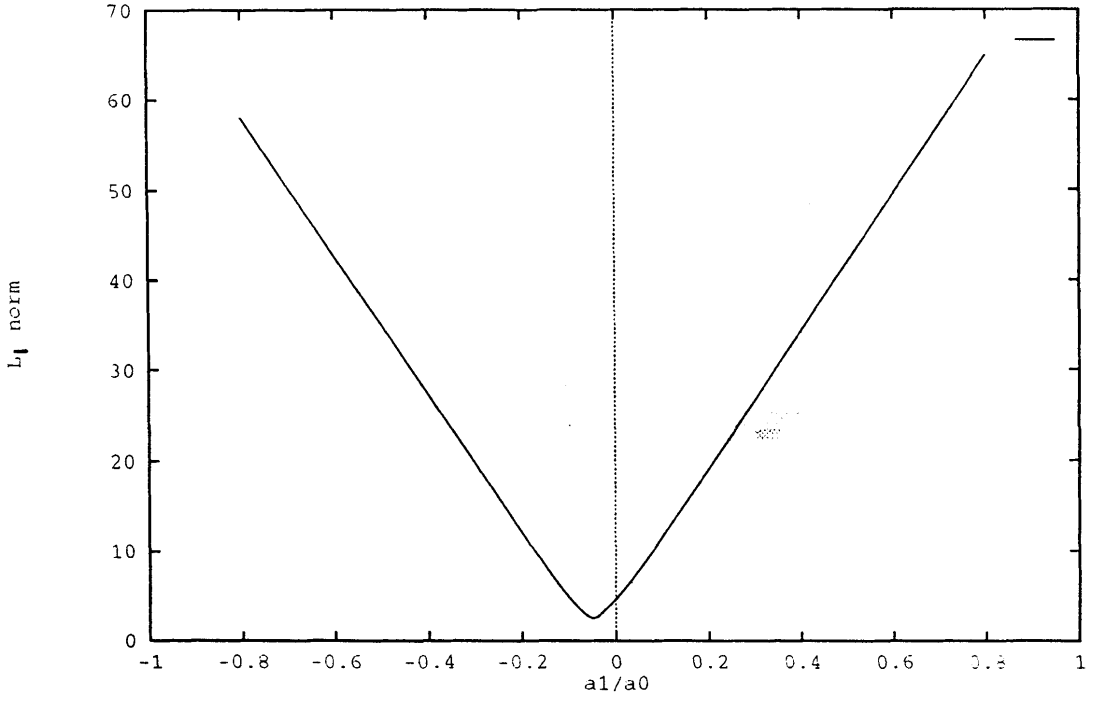

Figure 5: L_1 norm of the function $\psi \mapsto F(a_1/a_0, \psi)$ for various values of a_1/a_0

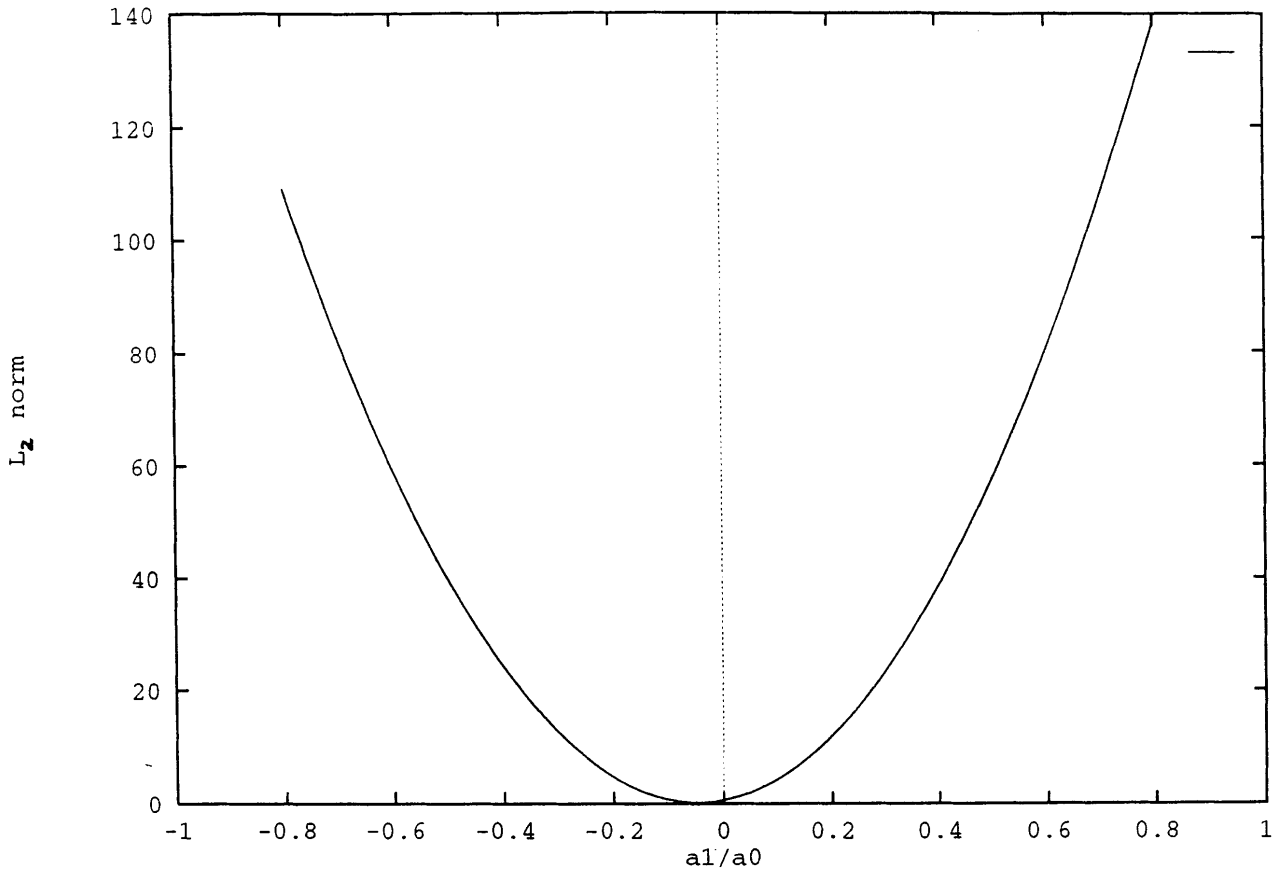

Figure 6: L_2 norm of the function $\psi \mapsto F(a_1/a_0, \psi)$ for various values of a_1/a_0

We can conclude that the optimum eigenvector $\vec{\mathbf{a}}$ is:

$$\vec{\mathbf{a}} = \begin{bmatrix} a_0 \\ a_1 \end{bmatrix} = a_0 \begin{bmatrix} 1 \\ -0.05 \end{bmatrix} \tag{29}$$

Thus we have $\vec{\mathbf{a}}$ with an arbitrary constant a_0, which in turn is determined by sampling the computed voltage at one point in the vicinity of the corner. That computed voltage is obtained from an initial finite-difference analysis of the given configuration of conductors.

We next discuss how $P_\alpha^0(\cos\theta)$ and $P_\alpha^{-3}(\cos\theta)$ was calculated. From [14, page 623] and

[1, page 556], for $-1 < z < 1$, we have

$$P_\nu^\mu(z) = \frac{1}{\Gamma(1-\mu)} \left[\frac{1+z}{1-z}\right]^{\frac{1}{2}\mu} F(-\nu, \nu+1; 1-\mu; \frac{1-z}{2}) \tag{30}$$

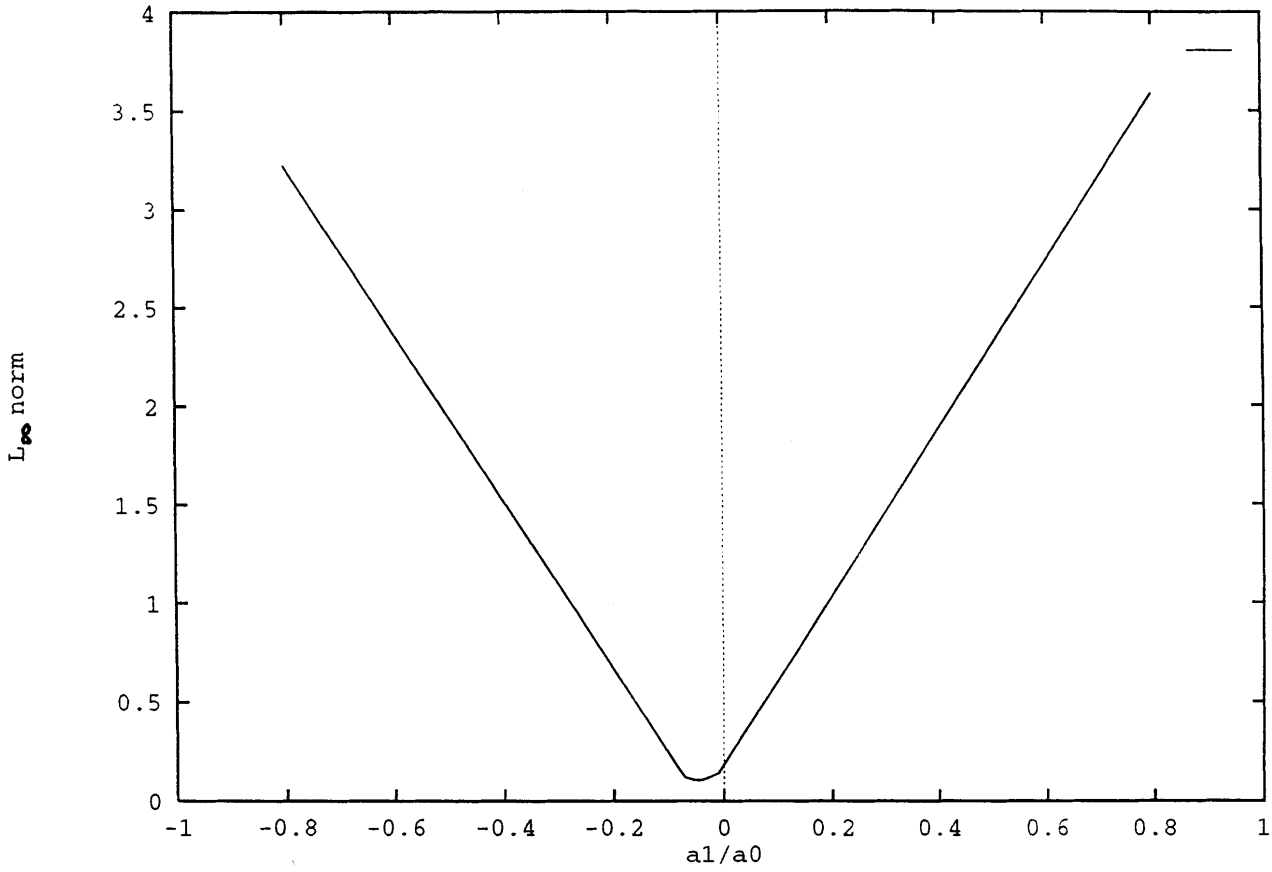

Figure 7: L_∞ norm of the function $\psi \mapsto F(a_1/a_0, \psi)$ for various values of a_1/a_0

and

$$F(a, b; c; z) = \sum_{n=0}^{\infty} \frac{(a)_n (b)_n}{(c)_n} \frac{z^n}{n!} \tag{31}$$

Note that Γ now denotes the standard Gamma function rather than the curve Γ of Figure 2. According to (30) and (31), we get

$$P_\alpha^0(\cos\theta) \;=\; F(-\alpha; \alpha+1; 1; \frac{1-\cos\theta}{2})$$

$$
\begin{aligned}
&= \sum_{n=0}^{\infty} \frac{(-\alpha)_n(\alpha+1)_n}{(1)_n n!}\left(\frac{1-\cos\theta}{2}\right)^n \\
&= \sum_{n=0}^{\infty} \frac{(-\alpha)_n(\alpha+1)_n}{(n!)^2}\left(\frac{1-\cos\theta}{2}\right)^n \\
&= \sum_{n=0}^{\infty} c_n\left(\frac{1-\cos\theta}{2}\right)^n \qquad (32)
\end{aligned}
$$

where F is now the hypergeometric series and

$$
\begin{aligned}
(a)_n &= a(a+1)(a+2)\ldots(a+n-1) \qquad n = 1,2,3\ldots. \\
c_0 &= 1 \\
c_1 &= (-\alpha)(\alpha+1)/(1!)^2 = c_0(-\alpha)(\alpha+1)/1^2 \\
c_2 &= (-\alpha)(-\alpha+1)(\alpha+1)(\alpha+2)/(2!)^2 = c_1(-\alpha+1)(\alpha+2)/2^2 \\
&\vdots \\
c_n &= c_{n-1}\frac{(-\alpha+n-1)(\alpha+n)}{n^2}
\end{aligned}
$$

The use of 130 terms in the summation (32) produces a convergence to within five significant figures . From (30) and (31), we obtain

$$
\begin{aligned}
P_\alpha^{-3}(\cos\theta) &= \frac{1}{\Gamma(4)}\left(\frac{1+\cos\theta}{1-\cos\theta}\right)^{-\frac{3}{2}} F(-\alpha;\alpha+1;4;\frac{1-\cos\theta}{2}) \\
&= \frac{1}{\Gamma(4)}\left(\frac{1+\cos\theta}{1-\cos\theta}\right)^{-\frac{3}{2}} \sum_{n=0}^{\infty} \frac{(-\alpha)_n(\alpha+1)_n}{(4)_n n!}\left(\frac{1-\cos\theta}{2}\right)^n \\
&= \left(\frac{1+\cos\theta}{1-\cos\theta}\right)^{-\frac{3}{2}} \sum_{n=0}^{\infty} \frac{(-\alpha)_n(\alpha+1)_n}{(n!)^2(n+3)(n+2)(n+1)}\left(\frac{1-\cos\theta}{2}\right)^n \\
&= \left(\frac{1+\cos\theta}{1-\cos\theta}\right)^{-\frac{3}{2}} \sum_{n=0}^{\infty} d_n\left(\frac{1-\cos\theta}{2}\right)^n \qquad (33)
\end{aligned}
$$

where

$$
\begin{aligned}
d_0 &= \frac{1}{6} \\
d_1 &= \frac{(-\alpha)(\alpha+1)}{(1!)^2\times 2\times 3\times 4} = \frac{1}{4\times 1}c_0(-\alpha)(\alpha+1) \\
d_2 &= \frac{(-\alpha)(-\alpha+1)(\alpha+1)(\alpha+2)}{(2!)^2\times 3\times 4\times 5} = \frac{1}{5\times 2}c_1(-\alpha+1)(\alpha+2)
\end{aligned}
$$

and n_3 are direction cosines of OZ, then we have

$$\begin{cases} x = l_1 X + l_2 Y + l_3 Z \\ y = m_1 X + m_2 Y + m_3 Z \\ z = n_1 X + n_2 Y + n_3 Z \end{cases} \tag{34}$$

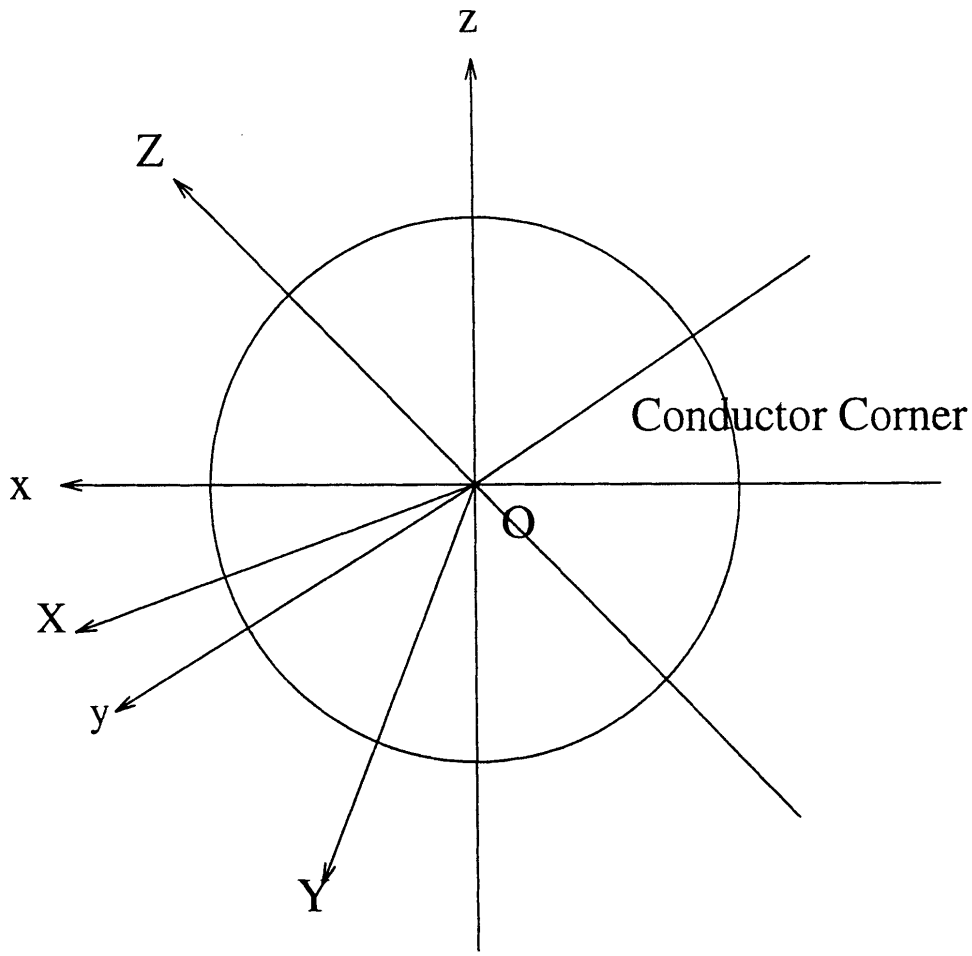

Figure 9: Rotation of coordinate system from that of Figure 8 to that of Figure 2. Again the conductor is in the octant $x < 0, y < 0, z < 0$.

The position of the new coordinate system can be determined by the three socalled Euler angles. We define these three angles as follows, also see Figure 10.

The colatitude angle θ_0 is the angle between OZ and Oz along the positive directions ($0 \leq$

$\theta_0 < \pi$).

The longitude angle ψ_0 is the angle between OA and Ox, viewed in the positive direction of the Oz axis, starting from the Ox axis in counterclockwise direction, where OA is the intersection line between OXY and Oxy ($0 \leq \psi_0 < 2\pi$).

The rotation angle ϕ_0 is the angle between OA and OX, viewed in the positive direction of OZ axis, starting from the OX axis in counterclockwise direction ($0 \leq \phi_0 \leq 2\pi$).

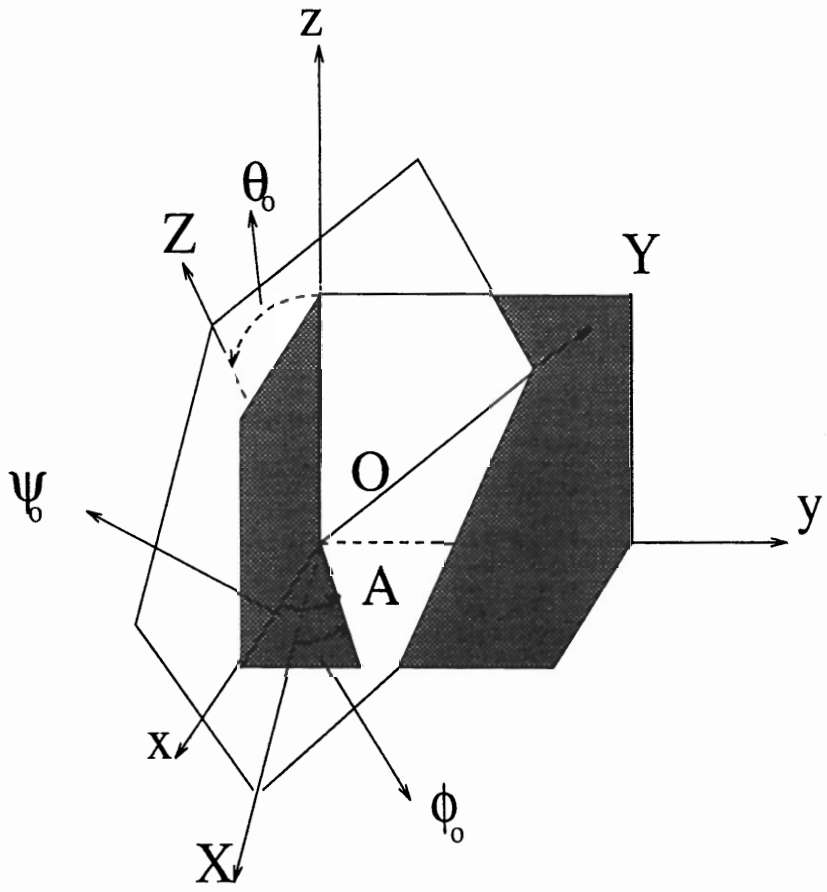

Figure 10: Relative positions of Euler angles

According to [34, page 331], we have the relationships between the direction cosines and the Euler angles as follows,

$$\begin{cases} l_1 = \cos\psi_0 \cos\phi_0 - \cos\theta_0 \sin\psi_0 \sin\phi_0 \\ l_2 = -\cos\psi_0 \sin\phi_0 - \cos\theta_0 \sin\psi_0 \cos\phi_0 \\ l_3 = \sin\theta_0 \sin\psi_0 \\ m_1 = \sin\psi_0 \cos\phi_0 + \cos\theta_0 \cos\psi_0 \sin\phi_0 \\ m_2 = -\sin\psi_0 \sin\phi_0 + \cos\theta_0 \cos\psi_0 \cos\phi_0 \\ m_3 = -\sin\theta_0 \cos\psi_0 \\ n_1 = \sin\theta_0 \sin\phi_0 \\ n_2 = \sin\theta_0 \cos\phi_0 \\ n_3 = \cos\theta_0 \end{cases}$$

In our problem, we have $\theta_0 = 54.73°$, $\psi_0 = 135°$, $\phi_0 = 30°$. Thus

$$\begin{cases} l_1 = -\sqrt{\frac{2}{3}} & m_1 = \frac{1}{\sqrt{6}} & n_1 = \frac{1}{\sqrt{6}} \\ l_2 = 0 & m_2 = -\frac{1}{\sqrt{2}} & n_2 = \frac{1}{\sqrt{2}} \\ l_3 = \frac{1}{\sqrt{3}} & m_3 = \frac{1}{\sqrt{3}} & n_3 = \frac{1}{\sqrt{3}} \end{cases} \tag{35}$$

Substituting (35) into (34), we get

$$\begin{cases} x = -\sqrt{\frac{2}{3}} X + \frac{1}{\sqrt{3}} Z \\ y = \frac{1}{\sqrt{6}} X - \frac{1}{\sqrt{2}} Y + \frac{1}{\sqrt{3}} Z \\ z = \frac{1}{\sqrt{6}} X + \frac{1}{\sqrt{2}} Y + \frac{1}{\sqrt{3}} Z \end{cases} \tag{36}$$

Therefore

$$\begin{cases} X = -\sqrt{\frac{2}{3}} x + \frac{1}{\sqrt{6}} y + \frac{1}{\sqrt{6}} z \\ Y = -\frac{1}{\sqrt{2}} y + \frac{1}{\sqrt{2}} z \\ Z = \frac{1}{\sqrt{3}} x + \frac{1}{\sqrt{3}} y + \frac{1}{\sqrt{3}} z \end{cases} \tag{37}$$

and also

$$\begin{cases} r = (X^2 + Y^2 + Z^2)^{\frac{1}{2}} \\ \phi = \arctan \frac{Y}{X} \\ \theta = \arctan \frac{(X^2+Y^2)^{\frac{1}{2}}}{Z} \end{cases} \tag{38}$$

Determination of the arbitary constant a_0: With (36) to (38) in hand, we can determine the arbitary constant a_0 of the eigenvector $\vec{\mathbf{a}}$. From (13) and (29), we have that

$$\begin{aligned} V(r,\theta,\phi) &= 1 + r^{.461}[a_0 P^0_{.461}(\cos\theta) + a_1 \cos 3\phi P^{-3}_{.461}(\cos\theta)] \\ &= 1 + a_0 r^{.461}[P^0_{.461}(\cos\theta) + (-0.05)\cos 3\phi P^{-3}_{.461}(\cos\theta)] \end{aligned} \tag{39}$$

We wish to use the sampled voltage located at a point near the corner in the diagonal direction along the Z coordinate, that is, at a point $\Delta x = \Delta y = \Delta z > 0$ in order to estimate the value of a_0. At first, we need to determine the spherical coordinates of this point. If we choose the origin of Oxyz at the apex of the corner, and $\Delta x = \Delta y = \Delta z = 0.5$ in the finite difference analysis, then the Oxyz coordinates for this point are x=0.5, y=0.5, z=0.5.

From (37), we have X=0, Y=0 and Z=0.8660. From (38), we get $r = 0.8660, \theta = 0°$ and $\phi = 0°$. From (32), (33) and $\cos\theta = 1$, $c_0 = 1$, we finally obtain $P^0_{.461}(\cos 0°) = 1$ and $P^{-3}_{.461}(\cos 0°) = 0$. Substituting these values into (39), we get

$$a_0 = r^{-.461}[V(r,\theta,\phi) - 1] = 1.06857[V(r,\theta,\phi) - 1] \tag{40}$$

Here $V(r,\theta,\phi)$ is obtained from our initial finite-difference analysis.

Corrected charge at a rectangular corner: We now calculate the charge at the corner. From (21) and (29), we have the charge density

$$\begin{aligned} \sigma(r,\theta,\phi) = -r^{-.539} a_0 \{1.461[\cos\theta P^0_{.461}(\cos\theta) - P^0_{1.461}(\cos\theta)] - 0.05\cos 3\phi \\ [1.461\cos\theta P^{-3}_{.461}(\cos\theta) - 4.461 P^{-3}_{1.461}(\cos\theta)]\}/\sin\theta \end{aligned} \tag{41}$$

The corrected charge at the corner is equal to the charge density σ integrated over the region shown in Figure 11. We can divide this region as region 1 and region 2 in Figures 12 and Figure 13. Region 1 is composed of three equal fanlike areas on the corner whose boundary is at r=.5, while the region 2 is the rest of the region shown in Figure 11. We will call the charge on region 1 as Q_1 and the charge on region 2 as Q_2.

Because of the symmetries of the region 1, to calculate Q_1 we only need integrate σ on one fanlike area. Furthermore, we only need to integrate σ on half that area. We call the

result Q_h: thus $Q_1 = 6Q_h$. For a more detailed explaination of this, see Appendix C. As for Q_h, from (41) we see that

$$Q_h = \int \sigma(r, \theta, \phi)\rho d\rho d\psi \tag{42}$$

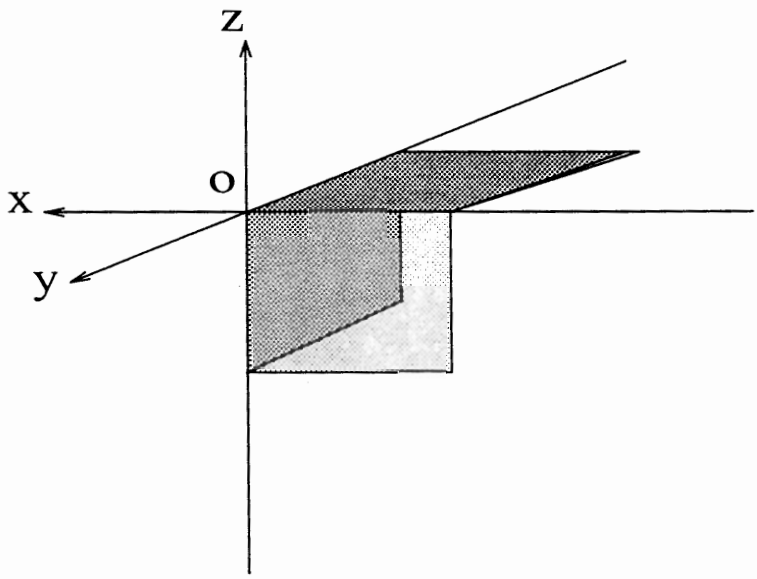

Figure 11: The incremental areas on a three-dimensional corner.

Note here that ψ is the same as in (24) and that (ρ, ψ) are the polar coordinates of the xy plane. So we have $x = \rho\cos\psi$, $y = \rho\sin\psi$. Substituting (37) into (38), we get

$$\begin{cases} r = (x^2 + y^2 + z^2)^{\frac{1}{2}} \\ \phi = \arctan \frac{\sqrt{3}(z-y)}{y+z-2x} \\ \theta = \arctan \sqrt{2}\frac{(x^2+y^2+z^2-xy-yz-zx)^{\frac{1}{2}}}{x+y+z} \end{cases} \tag{43}$$

In the Oxy plane, z=0. So from (43), we get $r = \rho$. Also note that by (24) , (42) becomes

$$\begin{aligned} Q_h &= \int \sigma(\rho, \psi)\rho d\rho d\psi \\ &= -a_0 \int_0^{0.5} \rho^{.461} d\rho \int_0^{\frac{\pi}{4}} F(\psi) d\psi \\ &= -0.2486 a_0 \int_0^{\frac{\pi}{4}} F(\psi) d\psi \end{aligned} \tag{44}$$

where

$$\begin{aligned} F(v) &= F(\theta,\phi) \\ &= \{1.461[\cos\theta P^{0}_{.461}(\cos\theta) - P^{0}_{1.461}(\cos\theta)] - 0.05\cos 3\phi \\ &\quad [1.461\cos\theta P^{-3}_{.461}(\cos\theta) - 4.461 P^{-3}_{1.461}(\cos\theta)]\}/\sin\theta \end{aligned} \tag{45}$$

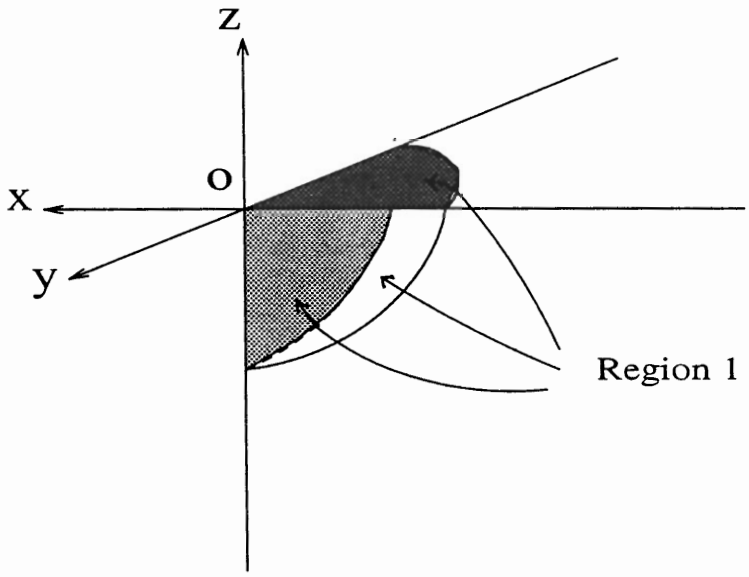

Figure 12: The three fan-like regions within the three incremental areas of Figure 11.

For the integral $\int_0^{\frac{\pi}{4}} F(\psi)d\psi$ in the (44) we incrementally integrate by using the trapezoidal rule with a uniform partition. According to that rule, we have

$$\begin{aligned} \int_a^b f(x)dx &= h[f(x_0)/2 + f(x_1) + \ldots + f(x_N)/2] \\ &= h[f(a)/2 + f(a+h) + \ldots + f(b-h) + f(b)/2] \end{aligned} \tag{46}$$

where $x_i = a + ih, i = 0, \ldots, N, x_N = b$.

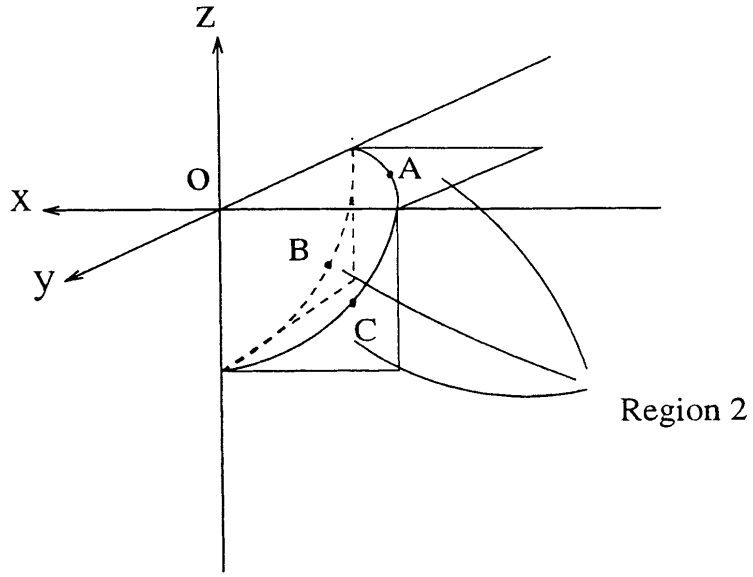

Figure 13: Region 2 beyond the fanlike region of the incremental areas.

In our problem, $x_0 = 0$ and $x_i = ih$, $x_N = \frac{\pi}{4}$. If we choose N=100, then $h = \frac{\pi}{400}$. Therefore, we have

$$\int_0^{\pi/4} F(\psi)d\psi = \frac{\pi}{400}\left[\frac{F(0)}{2} + F(\frac{\pi}{400}) + \ldots + F(\frac{\pi}{4} - \frac{\pi}{400}) + \frac{F(\frac{\pi}{4})}{2}\right] \tag{47}$$

Substituting (47) into (44), we get

$$Q_h = -0.00195a_0\left[\frac{F(0)}{2} + F(\frac{\pi}{400}) + \ldots + F(\frac{\pi}{4} - \frac{\pi}{400}) + \frac{F(\frac{\pi}{4})}{2}\right] \tag{48}$$

Therefore the charge on region 1 is

$$Q_1 = -0.01171a_0\left[\frac{F(0)}{2} + F(\frac{\pi}{400}) + \ldots + F(\frac{\pi}{4} - \frac{\pi}{400}) + \frac{F(\frac{\pi}{4})}{2}\right] \tag{49}$$

Next we calculate the charge Q_2 on region 2. Region 2 consists of three identical areas because of the symmetries of the region 2 (see Appendix C). Indeed we only need to compute the charge on the one of the three areas; let us indicate it by Q_t. Thus $Q_2 = 3Q_t$. In order to get Q_t, we need to get the charge density $\sigma(A)$ at the point A half-way along the curve Γ. Then $Q_t = \sigma(A) \times (0.5^2 - \frac{1}{4} \times \pi \times 0.5^2) = 0.05365\sigma(A)$. For the point A, we know that $x = -0.5\cos 45° = -0.3536, y = -0.5\cos 45° = -0.3536, z = 0$. From (37) and (38), we have the spherical coordinates of point A as follows:

$r = 0.5, \theta = 144.74°, \phi = 60°$. From (32) and (33), we get

$$P^0_{.461}(\cos 144.74°) = -.1817, \quad P^0_{1.461}(\cos 144.74°) = -.3295$$
$$P^{-3}_{.461}(\cos 144.74°) = 4.2590, \quad P^{-3}_{1.461}(\cos 144.74°) = 1.6770$$

Substituting these values into (21), we have $\sigma(A) = -0.1764a_0$. Therefore $Q_t = -0.0095a_0$. Thus we have

$$Q_2 = 3Q_t = -0.02839a_0 \tag{50}$$

Finally the corrected charge at a three-dimensional corner is

$$Q_c = Q_1 + Q_2 = -0.01171a_0 \left[\frac{F(0)}{2} + F(\frac{\pi}{400}) + \ldots + F(\frac{\pi}{4} - \frac{\pi}{400}) + \frac{F(\frac{\pi}{4})}{2}\right] - 0.02839a_0 \tag{51}$$

IV Numerical Results and Comparison

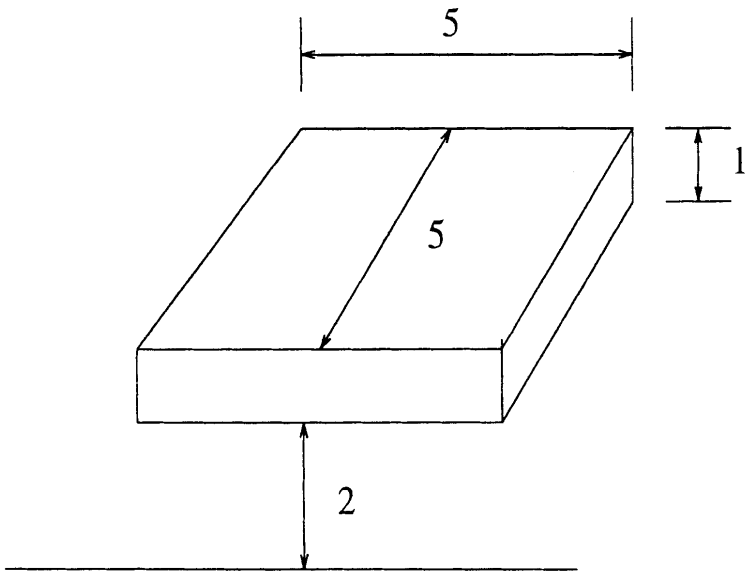

Figure 14: A rectangular conductor.

In order to verify the three-dimensional capacitance correction procedure and computational accuracy, several comparisons are made with exist data.

Example A

Consider the single conductor, shown in Figure 14, of 5 units length, 5 units width, 1 unit thickness and 2 units above a conducting silicon plane. If we ignore the singularities of the electrical field at corners and edges, but allow incremental areas of the finite-difference method to extend beyond edges, the value of capacitance C/ϵ_0 is 49.1F. If incremental areas extending beyond edges are deleted, the result is 34.8F. On the other hand, if we consider both factors, i.e., in the most accurate case where singularities are considered but extended areas are deleted, we get C/ϵ_0 equal to 41.8F. This result can be compared to the capacitance value given by Ruehli and Brennan in [23] by interpolating in their Fig.2. Their result is 42.5F.

Example B

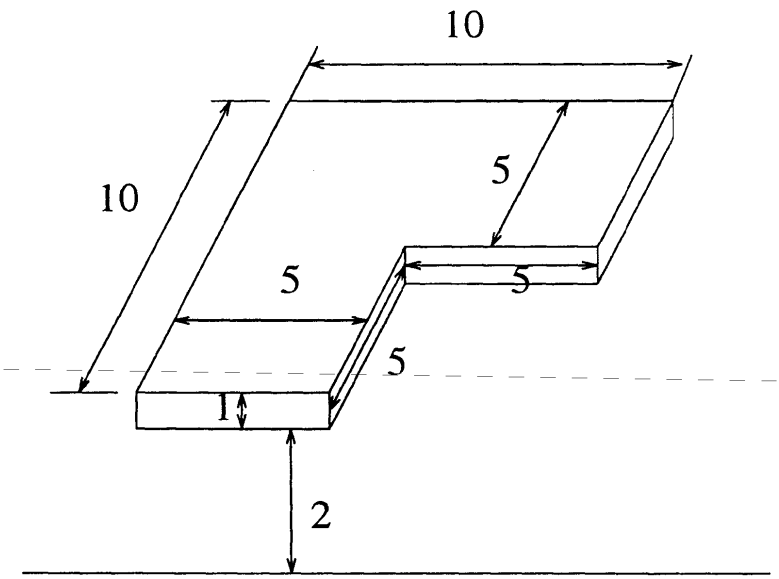

Figure 15: A right-angle three-dimensional bend.

Consider now a right-angle bend 2 units above a silicon chip. Its dimensions are shown in Figure 15. If we do not consider the singularity of the electrical field at corners and edges but allow overextending incremental areas, the value of capacitance C/ϵ_0 is 106.1F. If overextending areas are deleted, the result is 73.9F. On the other hand, if we correct both

factors. we get C/ϵ_0 is 83.1F. This result can be compared to the capacitance value given by Ruehli and Brennan in [20] by interpolating in their Fig.9; this value is 101.2F.

Appendix A

In this appendix, we will show that $V(r,\theta,\phi)$ in (12) is the solution of the Laplace equation. In the spherical polar coordinates, $\triangle V = 0$ becomes

$$\frac{\partial}{\partial r}(r^2\frac{\partial V}{\partial r}) + \frac{1}{\sin\theta}\frac{\partial}{\partial\theta}(\sin\theta\frac{\partial V}{\partial\theta}) + \frac{1}{\sin^2\theta}\frac{\partial^2 V}{\partial\phi^2} = 0 \tag{52}$$

Let $V(r,\theta,\phi) = R(r)U(\theta,\phi)$. After separating variables, we have

$$r\frac{d^2}{dr^2}(rR) - \alpha(\alpha+1)R = 0 \tag{53}$$

and

$$\left[\triangle^*_{\underline{\theta}} + \alpha(\alpha+1)\mathbf{I}\right] U(\underline{\theta}) = 0 \tag{54}$$

where $\mathbf{I}$ is the identity operator and $\triangle^*_{\underline{\theta}}$ is the Laplace-Beltrami operator defined as

$$\triangle^*_{\underline{\theta}} = \frac{1}{\sin\theta}\frac{\partial}{\partial\theta}(\sin\theta\frac{\partial}{\partial\theta}) + \frac{1}{\sin^2\theta}\frac{\partial^2}{\partial\phi^2} \tag{55}$$

where $\underline{\theta} = (\theta,\phi)$. In our problem $R(r) = r^\alpha$, $U(\underline{\theta}) = \sum_0^{N-1} a_n \cos 3n\phi P_\alpha^{-3n}(\cos\theta)$. It's obvious that R(r) satisfies (53). Therefore we only need to prove that

$$B_i^\alpha(\underline{\theta}) = a_n \cos 3n\phi P_\alpha^{-3n}(\cos\theta) \tag{56}$$

is the solution of (54), i.e.,

$$\left[\triangle^*_{\underline{\theta}} + \alpha(\alpha+1)\mathbf{I}\right] B_i^\alpha(\underline{\theta}) = 0 \tag{57}$$

Let us denote the left-hand side of (57) as L; then

$$\begin{aligned} L &= \frac{1}{\sin\theta}\frac{\partial}{\partial\theta}[\sin\theta\frac{\partial}{\partial\theta}B_i^\alpha(\underline{\theta})] + \frac{1}{\sin^2\theta}\frac{\partial^2 B_i^\alpha(\underline{\theta})}{\partial\phi^2} + \alpha(\alpha+1)B_i^\alpha(\underline{\theta}) \\ &= A + B + C \end{aligned} \tag{58}$$

where

$$\begin{aligned} B &= \frac{1}{\sin^2\theta}\frac{\partial^2 B_i^\alpha(\underline{\theta})}{\partial\phi^2} \\ &= \frac{1}{\sin^2\theta}\frac{\partial^2}{\partial\phi^2}[\cos 3n\phi P_\alpha^{-3n}(\cos\theta)] \\ &= \frac{1}{\sin^2\theta}P_\alpha^{-3n}(\cos\theta)(-9n^2)\cos 3n\phi \\ &= -\frac{9n^2}{\sin^2\theta}B_i^\alpha(\underline{\theta}) \end{aligned} \tag{59}$$

and

$$C = \alpha(\alpha+1)B_i^{\alpha}(\underline{\theta}) \tag{60}$$

Consider now the first term A. From [30, page 161], for $-1 < x < 1$, we have

$$\frac{dP_\nu^\mu(x)}{dx} = \frac{1}{1-x^2}[(\nu+1)xP_\nu^\mu - (\nu-\mu+1)P_{\nu+1}^\mu(x)] \tag{61}$$

Note here $x = \cos\theta$, we have

$$\begin{aligned}
\frac{\partial B_i^{\alpha}(\underline{\theta})}{\partial\theta} &= \frac{\partial}{\partial\cos\theta}\cos 3n\phi P_\alpha^{-3n}(\cos\theta)\frac{\partial\cos\theta}{\partial\theta} \\
&= -\sin\theta\cos 3n\phi\frac{1}{1-\cos^2\theta}\left[(\alpha+1)xP_\alpha^{-3n}(x) - (\alpha+3n+1)P_{\alpha+1}^{-3n}(x)\right] \\
&= -\frac{\cos 3n\phi}{\sin\theta}\left[(\alpha+1)xP_\alpha^{-3n}(x) - (\alpha+3n+1)P_{\alpha+1}^{-3n}(x)\right]
\end{aligned} \tag{62}$$

and therefore

$$\begin{aligned}
\frac{\partial}{\partial\theta}(\sin\theta\frac{\partial B_i^{\alpha}(\underline{\theta})}{\partial\theta}) &= \sin\theta\cos 3n\phi\frac{\partial}{\partial x}\left[(\alpha+1)xP_\alpha^{-3n}(x) - (\alpha+3n+1)P_{\alpha+1}^{-3n}(x)\right] \\
&= \sin\theta\cos 3n\phi\left[(\alpha+1)P_\alpha^{-3n}(x) + (\alpha+1)x\frac{dP_\alpha^{-3n}(x)}{dx} - (\alpha+3n+1)\frac{dP_{\alpha+1}^{-3n}(x)}{dx}\right] \\
&= \sin\theta\cos 3n\phi\left\{(\alpha+1)P_\alpha^{-3n}(x) + D - E\right\}
\end{aligned} \tag{63}$$

where we have

$$\begin{aligned}
D &= (\alpha+1)x\frac{dP_\alpha^{-3n}(x)}{dx} \\
&= \frac{(\alpha+1)x}{1-x^2}\left[(\alpha+1)xP_\alpha^{-3n}(x) - (\alpha+3n+1)P_{\alpha+1}^{-3n}(x)\right] \\
&= \frac{(\alpha+1)^2x^2P_\alpha^{-3n}(x)}{1-x^2} - \frac{(\alpha+1)(\alpha+3n+1)}{1-x^2}xP_{\alpha+1}^{-3n}(x)
\end{aligned} \tag{64}$$

and

$$\begin{aligned}
E &= (\alpha+3n+1)\frac{d}{dx}P_{\alpha+1}^{-3n}(x) \\
&= \frac{(\alpha+3n+1)}{1-x^2}\left[(\alpha+2)xP_{\alpha+1}^{-3n}(x) - (\alpha+3n+2)P_{\alpha+2}^{-3n}(x)\right]
\end{aligned} \tag{65}$$

From [34, page334], we have

$$(2\nu+1)xP_\nu^\mu(x) - (\nu-\mu+1)P_{\nu+1}^\mu(x) - (\nu+\mu)P_{\nu-1}^\mu(x) = 0 \tag{66}$$

Therefore

$$(\alpha+1+3n+1)P_{\alpha+2}^{-3n} = (2\alpha+3)xP_{\alpha+1}^{-3n}(x) - (\alpha+1-3n)P_{\alpha}^{-3n}(x) \tag{67}$$

Substituting (67) into (65), we get

$$\begin{aligned} E &= \frac{(\alpha+3n+1)}{1-x^2}\left[(\alpha+2)xP_{\alpha+1}^{-3n}(x) - (2\alpha+3)xP_{\alpha+1}^{-3n}(x) + (\alpha+1-3n)P_{\alpha}^{-3n}(x)\right] \\ &= \frac{(\alpha+3n+1)}{1-x^2}\left[(\alpha+1-3n)P_{\alpha}^{-3n}(x) - (\alpha+1)xP_{\alpha+1}^{-3n}(x)\right] \\ &= \frac{(\alpha+1)^2-9n^2}{1-x^2}P_{\alpha}^{-3n}(x) - \frac{(\alpha+1)(\alpha+3n+1)}{1-x^2}xP_{\alpha+1}^{-3n}(x) \end{aligned} \tag{68}$$

So, from (64) and (68), we have

$$D - E = \frac{(\alpha+1)^2x^2P_{\alpha}^{-3n}(x)}{1-x^2} - \frac{(\alpha+1)^2-9n^2}{1-x^2}P_{\alpha}^{-3n}(x) \tag{69}$$

From (63) and (69), we have

$$\begin{aligned} A &= \frac{1}{\sin\theta}\frac{\partial}{\partial\theta}(\sin\theta\frac{\partial B_i^{\alpha}(\underline{\theta})}{\partial\theta}) \\ &= \cos 3no\left[(\alpha+1)P_{\alpha}^{-3n}(x) + \frac{(\alpha+1)^2x^2P_{\alpha}^{-3n}(x)}{1-x^2} - \frac{(\alpha+1)^2-9n^2}{1-x^2}P_{\alpha}^{-3n}(x)\right] \\ &= \cos 3no\left[(\alpha+1)P_{\alpha}^{-3n}(x) - \frac{(\alpha+1)^2(1-x^2)}{1-x^2}P_{\alpha}^{-3n}(x) + \frac{9n^2}{1-x^2}P_{\alpha}^{-3n}(x)\right] \\ &= (\alpha+1)B_i^{\alpha}(\underline{\theta}) - (\alpha+1)^2B_i^{\alpha}(\underline{\theta}) + \frac{9n^2}{1-x^2}B_i^{\alpha}(\underline{\theta}) \end{aligned} \tag{70}$$

Finally, we have

$$\begin{aligned} L &= A + B - C \\ &= (\alpha+1)B_i^{\alpha}(\underline{\theta}) - (\alpha+1)^2B_i^{\alpha}(\underline{\theta}) + \frac{9n^2}{1-x^2}B_i^{\alpha}(\underline{\theta}) - \frac{9n^2}{1-x^2}B_i^{\alpha}(\underline{\theta}) + \alpha(\alpha+1)B_i^{\alpha}(\underline{\theta}) \\ &= 0 \end{aligned} \tag{71}$$

So we have showed that $V(r,\theta,\phi)$ in (12) is the solution of the Laplace equation.

Finally, let us note that $V(r,\theta,\phi)$ is only an asymptotic solution. This is because $V(r,\theta,\phi) \to \infty$ as r $\to \infty$ rather than $V(r,\theta,\phi) \to 0$ as r $\to \infty$. When r$\to$ 0, $V(r,\theta,\phi) \to 1$, as needed. So truly, $V(r,\theta,\phi)$ is only an asymptotic solution valid for $r \to 0$.

Appendix B

The purpose of his appendix is to show that (24) holds, i.e.,

$$\begin{cases} \cos\theta = -\sqrt{2/3}\sin(\psi + \pi/4) \\ \cos\phi = \frac{\sqrt{3}\cos\psi + \cos\theta}{\sqrt{2}\sin\theta} \qquad \psi \in [0,\ \pi/4] \end{cases} \tag{72}$$

From (37) in the paper, we have coordinate transforms as follows,

$$\begin{cases} X = -\sqrt{\frac{2}{3}}x + \frac{1}{\sqrt{6}}y + \frac{1}{\sqrt{6}}z \\ Y = -\frac{1}{\sqrt{2}}y + \frac{1}{\sqrt{2}}z \\ Z = \frac{1}{\sqrt{3}}x + \frac{1}{\sqrt{3}}y + \frac{1}{\sqrt{3}}z \end{cases} \tag{73}$$

and we also have

$$\begin{cases} X = r\sin\theta\cos\phi \\ Y = r\sin\theta\sin\phi \\ Z = r\cos\theta \end{cases} \tag{74}$$

and

$$\begin{cases} x = \rho\cos\psi \\ y = \rho\sin\psi \end{cases} \tag{75}$$

Assume that a point A on the curve Γ has coordinates(X, Y, Z) in the coordinate system OXYZ, and the coordinates (x, y, 0) in the coordinate system Oxyz. In the Oxy plane, we have $x = -\rho\cos\psi, y = -\rho\sin\psi$ for $\psi \in [0,\ \pi/4]$. Note $\rho = r$ for point on the curve Γ.

From (73) and (74) we have

$$\begin{cases} \sin\theta\cos\phi = \sqrt{\frac{2}{3}}\cos\psi - \frac{1}{\sqrt{6}}\sin\psi \\ \cos\theta = -\frac{1}{\sqrt{3}}\cos\psi - \frac{1}{\sqrt{3}}\sin\psi \end{cases} \tag{76}$$

Therefore, from the second equation we have $\cos\theta = -\sqrt{2/3}\sin(\psi + \pi/4)$. From the first equation we have $\cos\phi = \frac{\sqrt{3}\cos\psi + \cos\theta}{\sqrt{2}\sin\theta}$, where $\psi \in [0,\ \pi/4]$.

Appendix C

In this Appendix we explain the symmetries of the region 1 and the symmetries of the region 2.(See Figures 12, 13). We first examine region 1; it consists of three equal fanlike areas. To get the charge Q_1 we will integrate the charge density $\sigma(r, \theta, \phi)$ over these areas. Thus r, θ, ϕ must be expressed in terms of ρ and ψ, where that (ρ, ψ) are the polar coordinates of the Oxy plane, or Oyz plane, or Ozx plane. Substituting (37) into (38), we get the relationship between (r, θ, ϕ) and (x, y, z) as follows,

$$\begin{cases} r = (x^2 + y^2 + z^2)^{\frac{1}{2}} \\ \phi = \arctan \frac{\sqrt{3}(z-y)}{-2x+y+z} \\ \theta = \arctan \frac{\sqrt{2}(x^2+y^2+z^2-xy-xz-yz)^{\frac{1}{2}}}{x+y+z} \end{cases} \tag{77}$$

In the Oxy plane, $z = 0$ and (77) becomes

$$\begin{cases} r = (x^2 + y^2)^{\frac{1}{2}} \\ \phi = \arctan \frac{-\sqrt{3}y}{-2x+y} \\ \theta = \arctan \frac{\sqrt{2}(x^2+y^2-xy)^{\frac{1}{2}}}{x+y} \end{cases} \tag{78}$$

Note that we have $x = \rho \cos\psi$, $y = \rho \sin\psi$. Therefore (78) is

$$\begin{cases} r = \rho \\ \phi = \arctan \frac{\sqrt{3}\sin\psi}{2\cos\psi - \sin\psi} \\ \theta = \arctan \frac{\sqrt{2}(1-\cos\psi\sin\psi)^{\frac{1}{2}}}{\cos\psi+\sin\psi} \end{cases} \tag{79}$$

In the Oyz plane, $x = 0$ and (77) becomes

$$\begin{cases} r = (y^2 + z^2)^{\frac{1}{2}} \\ \phi = \arctan \frac{\sqrt{3}(z-y)}{z+y} \\ \theta = \arctan \frac{\sqrt{2}(y^2+z^2-yz)^{\frac{1}{2}}}{y+z} \end{cases} \tag{80}$$

Also note that we have $y = \rho \cos\psi$, $z = \rho \sin\psi$. Therefore (80) is

$$\begin{cases} r = \rho \\ \phi = \arctan \frac{\sqrt{3}\sin\psi - \cos\psi}{\sin\psi+\cos\psi} \\ \theta = \arctan \frac{\sqrt{2}(1-\cos\psi\sin\psi)^{\frac{1}{2}}}{\cos\psi+\sin\psi} \end{cases} \tag{81}$$

In the Ozx plane, $y = 0$ and (77) becomes

$$\begin{cases} r = (z^2 + x^2)^{\frac{1}{2}} \\ \phi = \arctan \frac{\sqrt{3}z}{z-2x} \\ \theta = \arctan \frac{\sqrt{2}(x^2+z^2-xz)^{\frac{1}{2}}}{x+z} \end{cases} \tag{82}$$

Finally note that we have $z = \rho\cos\psi$, $x = \rho\sin\psi$. Therefore (82) is

$$\begin{cases} r = \rho \\ \phi = \arctan \frac{\sqrt{3}\cos\psi}{\cos\psi - 2\sin\psi} \\ \theta = \arctan \frac{\sqrt{2}(1-\cos\psi\sin\psi)^{\frac{1}{2}}}{\cos\psi+\sin\psi} \end{cases} \tag{83}$$

From (79), (81) and (83), we can see that in the Oxy, Oyz, Ozx plane, r and θ are the same functions of (ρ, ψ), but ϕ is not. However, this will not make any difference when we integrate $\sigma(r, \theta, \phi)$ over the fanlike area in Oxy, Oyz and Ozx plane respectively. We can explain this point as follows.

If we locate three points on the Oxy, Oyz and Ozx plane respectively such that they have the same coordinate values (ρ, ψ), then by using above equations we can get the values of $\phi_{xy}, \phi_{yz}, \phi_{zx}$ for these three points.

$$\begin{cases} \tan\phi_{xy} = \frac{-\sqrt{3}y}{y-2x} \\ \tan\phi_{yz} = \frac{\sqrt{3}(z-y)}{z+y} = \frac{-\sqrt{3}(y-x)}{y+x} \\ \tan\phi_{zx} = \frac{\sqrt{3}z}{z-2x} = \frac{\sqrt{3}x}{x-2y} \end{cases} \tag{84}$$

Therefore,

$$\begin{aligned} \tan(\phi_{xy} - \phi_{yz}) &= \frac{\tan\phi_{xy} - \tan\phi_{yz}}{1 - \tan\phi_{xy}\tan\phi_{yz}} \\ &= \frac{\frac{-\sqrt{3}y}{y-2x} - \frac{\sqrt{3}(y-x)}{y+x}}{1 + \frac{-\sqrt{3}y}{y-2x}\frac{\sqrt{3}(y-x)}{y+x}} \\ &= \frac{-\sqrt{3}y(y+x) - \sqrt{3}(y-x)(y-2x)}{(y-2x)(y+x) - 3y(y-x)} \\ &= \frac{\sqrt{3}(-2y^2+2xy-2x^2)}{(-2y^2+2xy-2x^2)} \\ &= \sqrt{3} \end{aligned} \tag{85}$$

and

$$\begin{aligned}
\tan(\phi_{xy} - \phi_{zx}) &= \frac{\tan\phi_{xy} - \tan\phi_{zx}}{1 - \tan\phi_{xy}\tan\phi_{zx}} \\
&= \frac{\frac{-\sqrt{3}y}{y-2x} - \frac{\sqrt{3}x}{x-2y}}{1 + \frac{-\sqrt{3}y}{y-2x}\frac{-\sqrt{3}x}{x-2y}} \\
&= \frac{-\sqrt{3}y(x-2y) - \sqrt{3}x(y-2x)}{(y-2x)(x-2y) - 3xy} \\
&= \frac{-\sqrt{3}(-2y^2 + 2xy - 2x^2)}{(-2y^2 + 2xy - 2x^2)} \\
&= -\sqrt{3}
\end{aligned} \tag{86}$$

From (85) and (86), we get

$$\begin{cases} \phi_{xy} - \phi_{zx} = \frac{2\pi}{3} \\ \phi_{xy} - \phi_{yz} = \frac{4\pi}{3} \end{cases} \tag{87}$$

In the charge density (41), we only need 3ϕ. This means that

$$\begin{cases} 3(\phi_{xy} - \phi_{zx}) = 2\pi \\ 3(\phi_{xy} - \phi_{yz}) = 4\pi \end{cases} \tag{88}$$

Therefore, we conclude that these three fanlike areas have geometric symmetry as far as (41) is concerned; that is, charge density varies in exactly the same way on all these areas.

Furthermore we need to integrate σ on only half of a fanlike area to get Q_h and then $Q_1 = 6Q_h$. We can prove this as follows. For $\psi \in [0, \pi/4]$, we have

$$\begin{cases} \cos\theta = -\sqrt{2/3}\sin(\psi + \pi/4) \\ \cos\phi = \frac{\sqrt{3}\cos\psi + \cos\theta}{\sqrt{2}\sin\theta} \end{cases} \qquad \psi \in [0, \pi/4] \tag{89}$$

We can calculate $\int_{\frac{\pi}{4}}^{\frac{\pi}{2}} F(\psi)d\psi$ using the same method as given in the above section, *Corrected charge at a rectangular corner*. The only difference is that (θ, ϕ) is determined by (89) rather than by (24), where $F(\psi)$'s expression is the (45). When we implemented this calculation in the computer, we found that

$$\int_{\frac{\pi}{4}}^{\frac{\pi}{2}} F(\psi)d\psi = \int_0^{\frac{\pi}{4}} F(\psi)d\psi \tag{90}$$

Let us now exaimine the symmetries of region 2 shown in Figure 13. For the part of the region 2 in the Oxy plane, call the charge on it Q_{t1}. Let A be the point on Γ with the coordinates $(x, y. z) = (-.5\cos 45°, -.5\sin 45°, 0)$. Then we have

$$Q_{t1} = \sigma(A)(0.5^2 - \frac{1}{4}\pi^2) \tag{91}$$

For the part of the region 2 in the Oyz plane, call the charge on it Q_{t2}. Select a point B with the coordinates $(x, y, z) = (0, -.5\cos 45°, -.5\sin 45°)$. Then we have

$$Q_{t2} = \sigma(B)(0.5^2 - \frac{1}{4}\pi^2) \tag{92}$$

For the part of the region 2 in the Ozx plane, call the charge on it Q_{t3}. Select a point C with the coordinates $(x, y, z) = (-.5\cos 45°, 0, -.5\sin 45°)$. Then we have

$$Q_{t3} = \sigma(C)(0.5^2 - \frac{1}{4}\pi^2) \tag{93}$$

Using (37), (38) and (41), we get

$$\sigma(A) = \sigma(B) = \sigma(C) \tag{94}$$

Therefore

$$Q_{t1} = Q_{t2} = Q_{t3} = Q_t \tag{95}$$

and $Q_2 = 3Q_t$.

References

[1] M. Abramowitz, I. A. Stegun, "Handbook of Mathematical Functions with Formulas, Graphs and Mathematical Tables," U. S. Department of commerce; *National Bureau of standards Applied Marthematics Series 55.*

[2] Z. P. Bazant, " Three-dimensional harmonic function near termination or intersection of gradient singularity lines: A general numerical method," *International Journal of Engineering Sciences,* **12**(1974), pp. 221-243

[3] A. E. Beagles and J. R. Whiteman, "General conical singularities in three-dimensional Poisson problems," *Mathematical Methods in the Applied Sciences,* **11**(1989), pp. 215-235,

[4] A. E. Beagles and J. R. Whiteman, "Treatment of a re-entrant vertex in a three-dimensional Poisson problems,"in *Singularities and Constructive Methods for Their Treatment,* P.Grisvard, W. L. Wendland, and J. R. Whiteman(Editors), Lecture Notes in Mathematics, Springer-Verlag, 1983, pp. 19-27.

[5] W. H. Chang, "Analytic IC metal-line capacitance formulas," *IEEE Trans. Microwave Theory and Techniques,* **24**(1976), pp. 608-611; see also **25**(1977), 712.

[6] P. E. Cottrell, E. M. Buturla, and D. R. Thomas, " Multi-dimensional simulation of VLSI wiring capacitance," *International Electron Devices Meeting Technical Digest,* **IEDM – 82**(1982), pp. 548-551.

[7] J. W. Duncan, "The accuracy of finite-difference solutions of Laplace's equation," *IEEE Trans. Microwave Theory and Techniques,* **15**(1967), pp. 575-582.

[8] R. L. M. Dang and N. Shigyo, "Coupling capacitances for two-dimensional wires," *IEEE Electron Devices Letters,* **2**(1981), pp. 196-197.

[9] M. I. Elmasry, "Capacitance calculations in MOSFET VLSI," *IEEE Electron Devices Letters,* **3**(1982), pp. 6-7.

[10] A. Erdelyi, *Higher Transcendental Functions,* Voll, McGraw-HILL Book Company, Inc. 1953.

[11] G. Fichera, "Asymptotic behaviour of the electric field and of the electric density near the singular points of the conductor surface," (in Russian), *Uspekhi Matematicheski Nauk,* **30**(1970), pp. 105-124.

[12] G. Fichera, "Asymptotic behaviour of the electric field near the singular points of the conductor surface," *Atti. accad. Naz Lincei Rend. Cl. Sci. Fis. Mat. Natur.,Series 8,* **60**(1976), pp. 13-20.

[13] G. Fichera and M. A. S. Ludovici, "Distribution de la charge electrique dans le voisinage des sommets et des aretes d'un cube," *C. R. Acad. Sc. Paris, Series A,* **278**(1974), pp. 1303-1306.

[14] Handbook of Mathematics, *Publisher of people's education, P. R. China* Dec. 1977.

[15] D. W. Kammler, "Calculation of characteristic admittances and coupling coefficients for strip transmission lines," *IEEE Trans. Microwave Theory and Techniques,***16**(1968), pp. 925-927.

[16] L. M. Keer and K. S. Parihar, "A note on the singularity at the corner of a wedge-shaped punch or crack," *SIAM J. Appl. Math.,* **34**(1978), pp. 297-302.

[17] T. Kitazawa and Y. Hayashi, "Asymmetrical three-line coupled striplines with anistropic substrates," *IEEE Trans. Microwave Theory and Techniques,* **34**(1986), pp. 767-772.

[18] V. A. Kondriatev and O. A. Oleinik, "Boundary-value problems for partial differential equations in non-smooth domains," *Russian Mathematical Surveys,* **38**(1983), pp. 1-86.

[19] J. A. Morrison and J. A. Lewis, "Charge Singularity at the corner of a flat plate," *SIAM J. Appl. Math.,* **31**(1976), pp. 233-250.

[20] Z. Q. Ning, P. M. Dewilde and F. L. Neerhoff, "Capacitance coefficients for VLSI multilevel metallization lines," *IEEE Trans. Electron Devices.* **34**(1987), pp. 644-649.

[21] P. D. Patel. "Calculation of capacitance coefficients for a system of irregular finite conductors on a dielectric sheet, " *IEEE Trans. Microwave Theory and Techniques*, **19**(1971), pp. 862-869.

[22] A. E. Ruehli. "Survey of computer-aided electrical analysis of integrated circuits interconnections." *IBM Journal of Research and Development* **23**(1979), pp. 626-639.

[23] A. E. Ruehli and P. A. Brennan, "Accurate metallization capacitances for integrated circuits and packages," *IEEE Journal of Solid-State Circuits*, **8**(1973), pp. 289-290.

[24] A. E. Ruehli and P. A. Brennan, "Capacitance models for integrated circuit metallization wires," *IEEE Journal of Solid-State Circuits*. **10**(1975), pp. 530-536.

[25] T. Sakarai and K. Tamaru, "Simple formulas for two- and three- dimensional capacitances," *IEEE Trans. Electron Devices*, **30**(1983), pp. 183-185.

[26] E. Stephan, J. R. Whiteman, "Singularities of the Laplacian at Corners and Edges of Three-Dimensional Domains and Their Treatment with Finite Element Methods," *Mathmatical Methods in the Applied Sciences*, **Vol.10** (1988), pp.339-350.

[27] C. D. Taylor, G. N. Elkhouri and T. E. Wade, "On the parasitic capacitances of multilevel parallel metallization lines," *IEEE Trans. Electron Devices*, **32**(1985), pp. 2408-2414.

[28] J.Venkatraman, T. K. Sarkar, S. M. Rao, A. R. Djordjevic and Y. Naiheng, "Analysis of arbitrarily oriented microstrip transmission lines in arbitrarily shaped dielectric media over a finite ground plane," *IEEE Trans. Microwave Theory and Techniques*, **33**(1985), pp. 952-959.

[29] W. T. Weeks. "Calculation of coefficients of capacitances of multiconductor transmission lines in the presence of a dielectric interface," *IEEE Trans. Microwave Theory and Techniques*, **18**(1970), pp. 35-43.

[30] C. Wei, R. F. Harrington, J.R. Mautz and T. K. Sarkar, "Multiconductor transmission lines in multilayered dielectric media," *IEEE Trans. Microwave Theory and Techniques*, **32**(1984), pp. 439-450.

[31] N. M. Wigley, "An efficient method for subtracting off singularities at corners for Laplace's equation," *J. Computational Physics,* **78**(1988), pp. 369-377.

[32] A. H. Zemanian, " A finite-difference procedure for the exterior problem inherent in capacitance computations for VLSI interconnections," *IEEE Trans. Electron Devices,* **35**(1988), pp. 985-992.

[33] A. H. Zemanian, *Infinite electrical networks,* Cambridge University Press, England, 1991.

[34] A. H. Zemanian, P. R. Tewarson, C. P. Ju and J. F. Jen, "Three-dimensional capacitance computations for VLSI/ULSI interconnections," *IEEE Trans. Computer-Aided Design,* **8**(1989), pp. 1319-1326.